



Article

Design of Deep Eutectic Systems: Plastic Crystalline Materials as Constituents

Ahmad Alhadid ^{1,*} , Sahar Nasrallah ¹, Liudmila Mokrushina ² and Mirjana Minceva ¹ 

¹ Biothermodynamics, TUM School of Life Sciences, Technical University of Munich (TUM), Maximus-von-Imhof-Forum 2, 85354 Freising, Germany

² Separation Science & Technology, Friedrich-Alexander-Universität Erlangen-Nürnberg (FAU), Egerlandstr. 3, 91058 Erlangen, Germany

* Correspondence: ahmad.alhadid@tum.de; Tel.: +49-8161-71-6173

Abstract: Deep eutectic solvents (DESs) are a class of green and tunable solvents that can be formed by mixing constituents having very low melting entropies and enthalpies. As types of materials that meet these requirements, plastic crystalline materials (PCs) with highly symmetrical and disordered crystal structures can be envisaged as promising DES constituents. In this work, three PCs, namely, neopentyl alcohol, pivalic acid, and neopentyl glycol, were studied as DES constituents. The solid–liquid transitions and melting properties of the pure PCs were studied using differential scanning calorimetry. The solid–liquid equilibrium phase diagrams of four eutectic systems containing the three PCs, i.e., L-menthol/neopentyl alcohol, L-menthol/pivalic acid, L-menthol/neopentyl glycol, and choline chloride/neopentyl glycol, were measured. Despite showing near-ideal behavior, the four studied eutectic systems exhibited depressions at the eutectic points, relative to the melting temperatures of the pure constituents, that were similar to or even larger than those of strongly nonideal eutectic systems. These findings highlight that a DES can be formed when PCs are used as constituents, even if the eutectic system is ideal.

Keywords: deep eutectic solvents; green solvents; solid–solid transition; solid–liquid equilibria; melting properties; differential scanning calorimetry



Citation: Alhadid, A.; Nasrallah, S.; Mokrushina, L.; Minceva, M. Design of Deep Eutectic Systems: Plastic Crystalline Materials as Constituents. *Molecules* **2022**, *27*, 6210. <https://doi.org/10.3390/molecules27196210>

Academic Editor: Mara G. Freire

Received: 27 August 2022

Accepted: 19 September 2022

Published: 21 September 2022

Publisher's Note: MDPI stays neutral with regard to jurisdictional claims in published maps and institutional affiliations.



Copyright: © 2022 by the authors. Licensee MDPI, Basel, Switzerland. This article is an open access article distributed under the terms and conditions of the Creative Commons Attribution (CC BY) license (<https://creativecommons.org/licenses/by/4.0/>).

1. Introduction

Deep eutectic solvents (DESs) are eutectic systems prepared by mixing two or more compounds to form a mixture with a melting temperature significantly lower than that of the individual constituents [1,2]. As a new generation of designer and green solvents, DESs are promising alternatives for overcoming the drawbacks of conventional solvents—particularly, their toxicity and environmental impacts [3–5]. Various DESs have been reported as potential green solvents that outperform conventional organic solvents in extraction, separation processes, and bioapplications [6–12].

For various applications, DESs must be liquid at the operating temperature. The solid–liquid equilibrium (SLE) phase diagram of DESs allows for identifying the melting temperature of the system at any composition. The SLE phase diagram and the position of the eutectic point depend on the nonideality of the liquid phase, the melting properties of the pure components, and the type of the formed solid phases [13].

In fact, the term DES is only applied for eutectic systems showing a substantial negative deviation from ideal behavior, i.e., strong hydrogen bonding interactions [14]. In many cases, mixing halide salts as hydrogen bond acceptors (HBAs) with carboxylic acids [15–17], polyols [18], sugars [19], sugar alcohols [20], or amides [21,22] as hydrogen bond donors (HBDs) results in the formation of eutectic systems with a substantial negative deviation from ideality and a low eutectic temperature. Accordingly, many studies regarding the SLE of DESs have focused on ionic constituents as HBAs. Nevertheless, the applicability of ionic DESs is somewhat restricted due to their high hygroscopicity, their thermal instability,

and the toxicity of some halide salts [23]. Moreover, the strong electrostatic interactions occurring in the liquid phase endow ionic DESs with viscosity and a high density [24–28].

To overcome the main drawbacks of ionic DESs, particularly their toxicity and hygroscopicity, natural organic compounds have recently been suggested as constituents of hydrophobic nonionic eutectic systems [29–32]. Simple organic compounds have been used to prepare nonionic eutectic systems that were found to be superior to ionic DESs and ionic liquids in terms of viscosity, economy, and performance [33,34]. However, because most nonionic eutectic systems studied in the literature are nearly ideal mixtures, their eutectic temperature is not significantly lower than the melting temperatures of the pure constituents [6,35]. To construct eutectic systems with a large depression in the melting temperature at the eutectic point, mixing components that have low melting entropies and enthalpies is an effective strategy [36]. For instance, constituents with rigid and symmetrical molecular structures have been shown to possess sufficiently low melting entropies to form eutectic systems with low eutectic temperatures [35].

The present work studies plastic crystalline materials (PCs) as constituents of eutectic systems with low eutectic temperatures. PCs are solid compounds with disordered and symmetrical crystal structures, i.e., a cubic lattice, and thus they possess extremely low melting entropies and enthalpies. Due to their unique mechanical and conducting properties, PCs have been used in various applications [37,38]. In this study, three PCs that have the chemical nature of commonly used DES constituents, namely, monocarboxylic acids, alcohols, and diols, were investigated. The three PCs were mixed with L-menthol or choline chloride (ChCl) to form four eutectic systems. The solid–plastic transition and melting properties of the pure PCs and the SLE phase diagram of the four eutectic systems were measured using differential scanning calorimetry (DSC). The SLE phase diagram was modeled to obtain the position of the eutectic point of the system.

2. Results and Discussion

2.1. Properties of Pure PCs

Due to their symmetrical crystal structure, PCs exhibit an extremely low melting entropy. Timmermans [39] reported an upper limit of $5 \text{ kcal mol}^{-1} \text{ K}^{-1}$ ($\sim 2.5 R$) for the melting entropies of PCs. As a result of their very small melting entropies, PCs tend to have higher melting temperatures than their chemical isomers. Figure 1 shows a comparison between the melting properties of various pentyl (C5) alcohol (Figure 1A), monocarboxylic acid (Figure 1B), and diol (Figure 1C) chemical isomers. As seen in Figure 1A, the melting temperatures of linear C5 alcohols (1-, 2-, and 3-pentanol) are similar. In contrast, tert-amyl and neopentyl alcohols exhibit significantly higher melting temperatures. Neopentyl alcohol is the only C5 alcohol that is solid at room temperature. Similarly, the melting temperature of pivalic acid (Figure 1B) and neopentyl glycol (Figure 1C) are significantly higher than those of their chemical isomers. The melting entropies of tert-amyl alcohol, neopentyl alcohol, pivalic acid, and neopentyl glycol are below Timmermans' limit, indicating that these compounds are PCs.

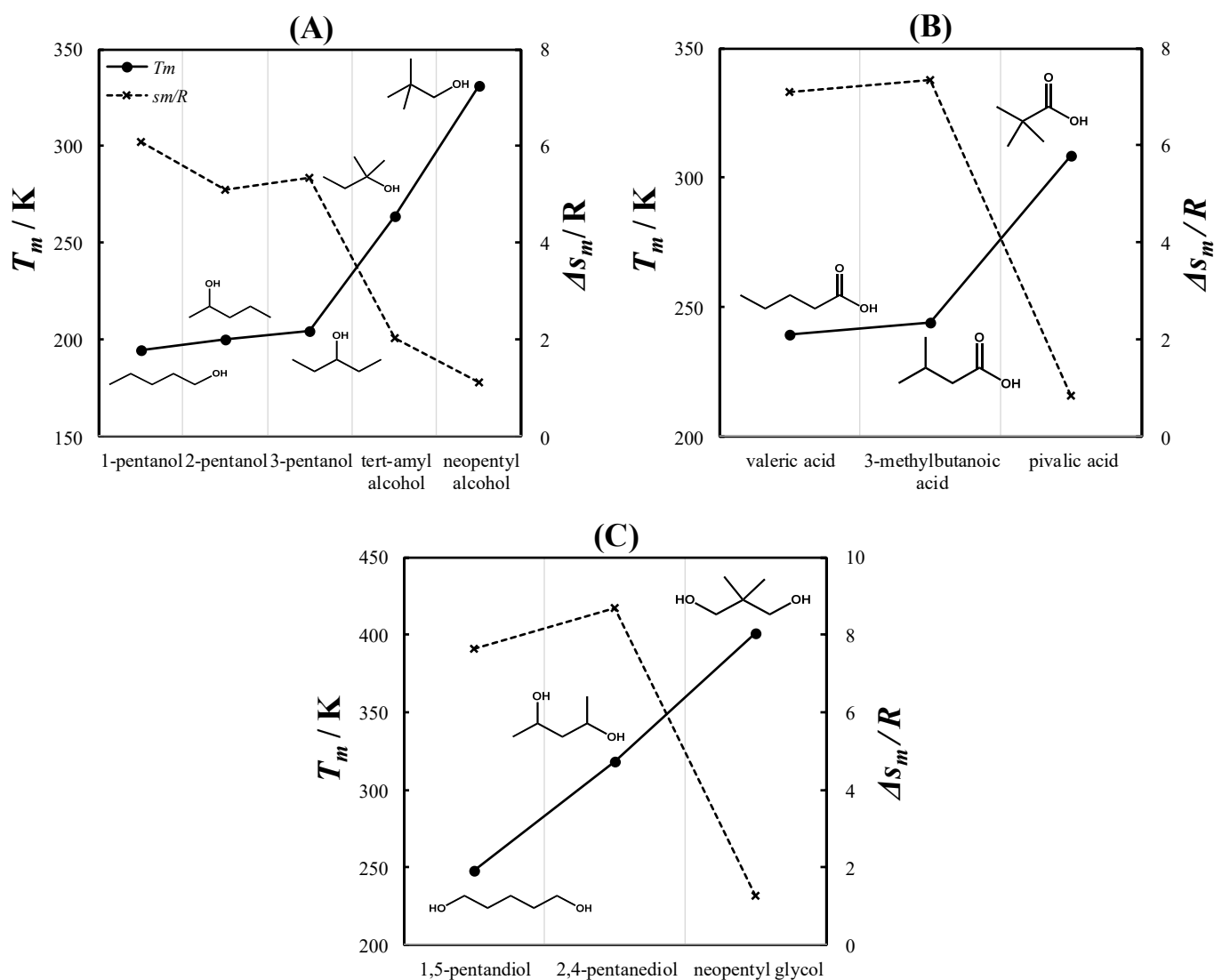


Figure 1. Melting temperatures (T_m) and melting entropies ($\Delta S_m/R$) of various isomers of C5 alcohols (A), monocarboxylic acids (B), and diols (C). Experimental data were taken from Lohmann et al. [40] for 1-, 2-, and 3-pentanol; Parks et al. [41] for tert-amyl alcohol; Timmermans [42] for valeric and 3-methylbutanoic acid; Miller [43] for 1,5-pentandiol; and Mellan [44] for 2,4-pentandiol. The melting entropies of 3-methylbutanoic acid and 2,4-pentandiol are unavailable in the literature and were estimated using the method of Jain et al. [45].

Upon cooling, PCs transform from high-symmetry disordered solid states (plastic states) to low-symmetry ordered solid states [37]. The solid–plastic transition can occur in a single or several phase transitions, and the associated enthalpy is larger than the plastic–liquid transition, i.e., the melting [39,46]. Figure 2 shows the DSC curves of the studied PCs, namely, neopentyl alcohol, pivalic acid, and neopentyl glycol. As seen in Figure 2, a single solid–plastic transition was observed. The solid–plastic transition (first peak) enthalpy was larger than the melting enthalpy (second peak). The largest difference between the solid–plastic transition and melting temperatures was observed in neopentyl alcohol, and the largest difference between the solid–plastic transition and melting enthalpies was found for neopentyl glycol.

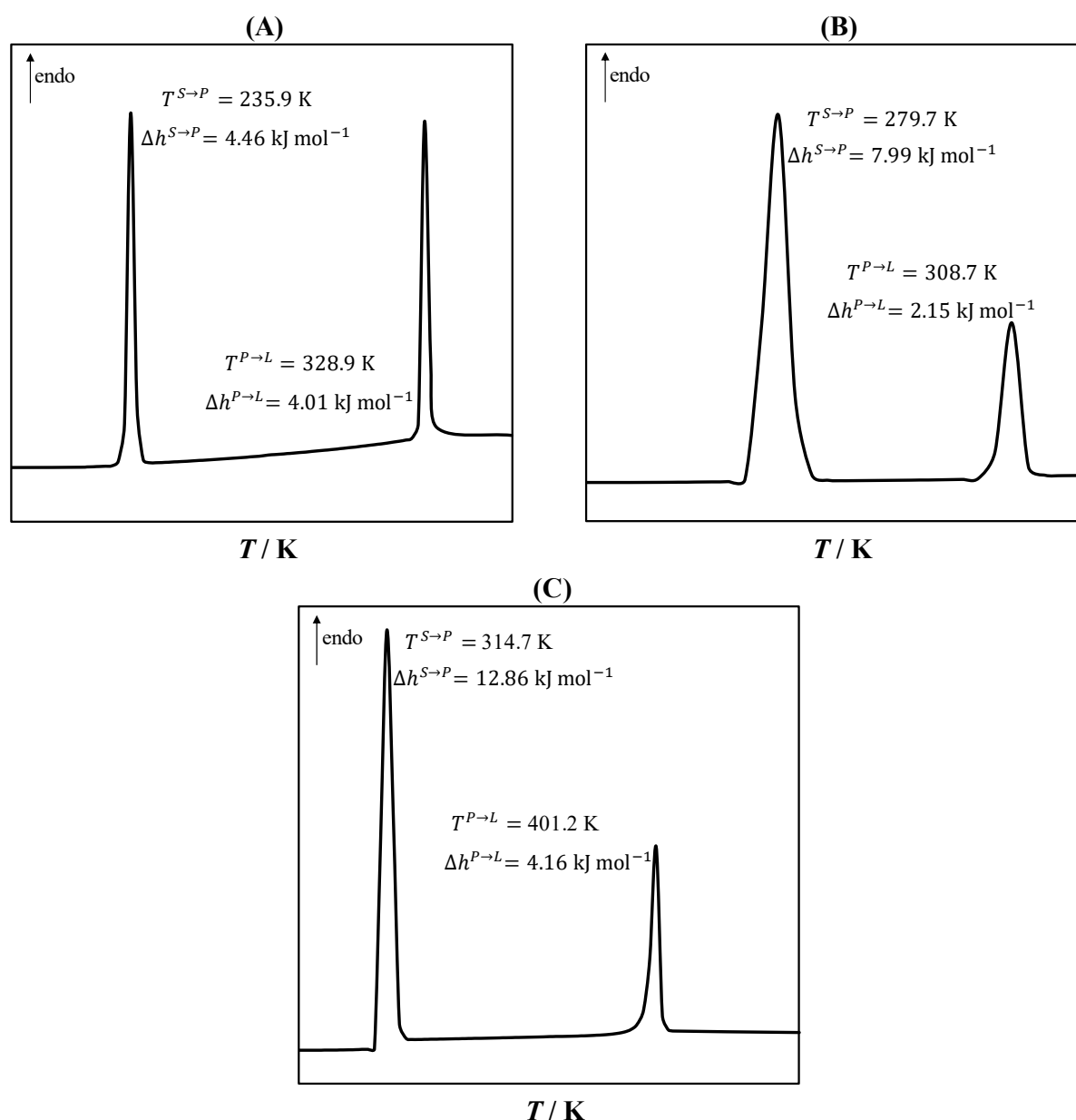


Figure 2. Differential scanning calorimetry curves of neopentyl alcohol (A), pivalic acid (B), and neopentylglycol (C), showing the solid–plastic transition temperature ($T^{S\rightarrow P}$) and enthalpy ($\Delta h^{S\rightarrow P}$) and the melting temperature ($T^{P\rightarrow L}$) and enthalpy ($\Delta h^{P\rightarrow L}$).

2.2. Eutectic Systems with PCs

In this work, the SLEs of three eutectic systems containing L-menthol and PCs were determined using DSC. Figure 3 shows the SLE phase diagram of L-menthol/neopentyl alcohol, L-menthol/pivalic acid, and L-menthol/neopentyl glycol.

No eutectic temperature for the L-menthol/neopentyl alcohol eutectic system (Figure 3A) could be measured due to the kinetic limitations in crystallization. The measured SLE data of the L-menthol liquidus line in the range of $x_{\text{alcohol}} < 0.3$ indicated that the system behaves ideally. Moreover, due to the similar chemical nature of L-menthol and neopentyl alcohol, i.e., both are alcohols, the liquid solution is expected to be ideal. Therefore, the eutectic temperature was estimated using the ideal solution model as 259.2 K. The solid–plastic transition of neopentyl alcohol did not influence the SLE phase diagram of the system because the solid–plastic transition temperature was lower than the eutectic temperature of the system.

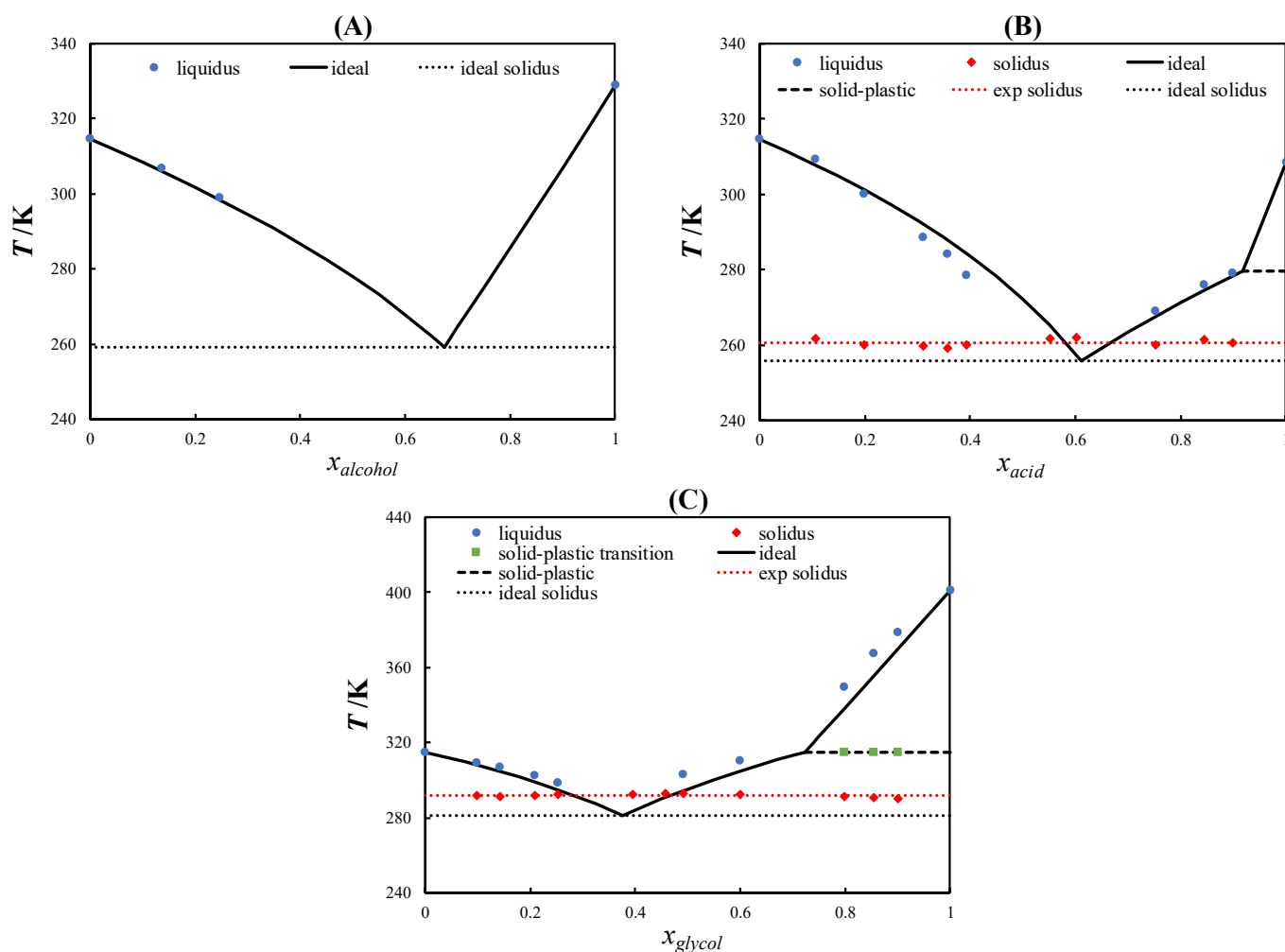


Figure 3. Solid–liquid phase diagram of L-menthol/neopentyl alcohol (A), L-menthol/pivalic acid (B), and L-menthol/neopentyl glycol (C).

As can be observed in the SLE phase diagram of the L-menthol/pivalic acid eutectic system shown in Figure 3B, the L-menthol liquidus line showed a slight negative deviation from the ideal behavior similar to that observed in L-menthol-based eutectic systems containing other monocarboxylic acids [35]. Meanwhile, the pivalic acid liquidus line showed a slightly positive deviation from the ideal behavior. Correspondingly, the eutectic temperature of the system was slightly higher than the ideal eutectic temperature.

Figure 3C displays the SLE phase diagram of the L-menthol/neopentyl glycol eutectic system, which exhibited a slightly positive deviation from the ideal behavior in the liquidus lines of L-menthol and neopentyl glycol. Accordingly, the eutectic temperature was higher than the ideal eutectic temperature. However, the difference between the eutectic temperature of the system and the melting temperature of neopentyl glycol was approximately 110 K, which is considerably high for a nearly ideal eutectic system.

As seen in Figure 3B,C, the course of the liquidus lines of pivalic acid and neopentyl glycol above the solid–plastic transition temperature was very steep due to the small melting enthalpies of the PCs. The slope of the liquidus line of the PCs decreased significantly below the solid–plastic transition temperature due to the relatively large solid–plastic transition enthalpy compared with the melting enthalpy. The order of the depression at the eutectic point relative to the melting temperature of the pure constituents was L-menthol/neopentyl alcohol > L-menthol/neopentyl glycol > L-menthol/pivalic acid, which was consistent with the difference between the solid–plastic transition and melting temperatures of the pure PCs (see Figure 2). Thus, the large difference between the solid–

plastic transition and melting temperatures resulted in a more significant depression at the eutectic point.

ChCl-based eutectic systems containing diols, such as ChCl/ethylene glycol, have been studied extensively [18,47–50]. Owing to the low melting temperature and slightly negative deviation from the ideal behavior of most diols, a small depression at the eutectic point is observed in ChCl-based eutectic systems containing diols [18,51,52]. In this work, neopentyl glycol, which possesses a high melting temperature, was mixed with ChCl. Figure 4 shows the SLE phase diagram of the ChCl/neopentyl glycol eutectic system. ChCl is thermally unstable and its melting properties cannot be measured or estimated indirectly [13]. Thus, the ChCl liquidus line could not be calculated. The eutectic temperature was significantly lower than the melting temperature of pure neopentyl glycol (~96 K). Despite the slightly negative deviation from the ideal solution behavior, a large depression at the eutectic point was observed in the system.

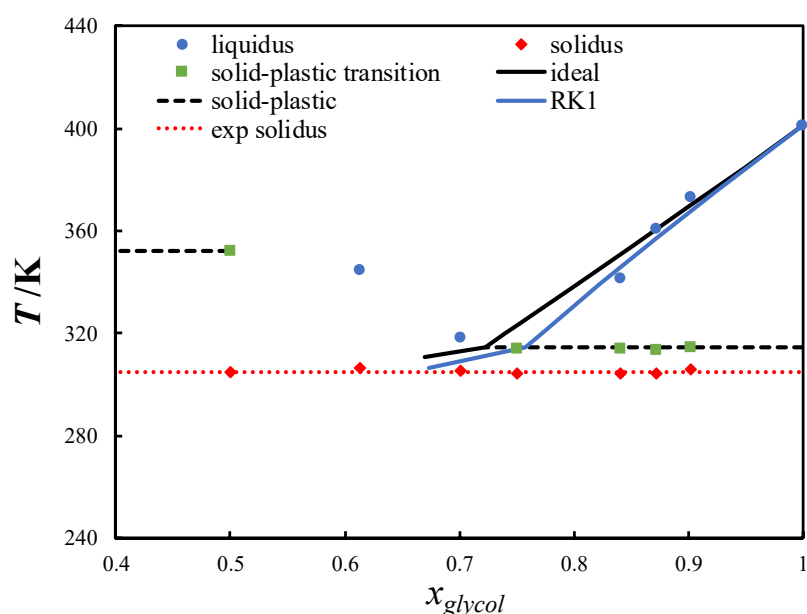


Figure 4. Solid–liquid phase diagram of the choline chloride/neopentyl glycol eutectic system. The black line is the ideal liquidus line of neopentyl glycol, and the blue line was calculated using the Redlich–Kister polynomial equation with one parameter (RK1).

2.3. Comparison with Other Eutectic Systems

The eutectic systems studied in this work exhibited very low eutectic temperatures compared with the melting temperatures of the pure constituents. Table 1 compares the experimental eutectic temperatures and the differences between the eutectic temperatures and the melting temperatures of plastic or common solid materials ($T_e^{exp} - T_{m,2}$) in various eutectic systems. First, three L-menthol-based eutectic systems containing monocarboxylic acids, namely, L-menthol/pivalic acid, L-menthol/cyclohexane carboxylic acid, and L-menthol/capric acid, are compared. The three eutectic systems are ideal mixtures [35], among which L-menthol/pivalic acid possesses the lowest eutectic temperature and the largest depression at the eutectic point. Thus, when selecting eutectic system constituents from a pool of substances sharing similar chemical natures, PCs can be expected to form deeper eutectics.

Table 1. A comparison between the melting temperatures of pure constituents (T_m), the experimental eutectic temperatures (T_e^{exp}), and the depressions at the eutectic points relative to the melting temperatures ($T_e^{exp} - T_{m,2}$) of the pure constituents of eutectic systems studied in this work and found in the literature.

Component 1	Component 2	$T_{m,2}/K$	T_e^{exp}/K	$(T_e^{exp} - T_{m,2})/K$
L-menthol	Pivalic acid ^{a,b}	308.7	260.6	−48.1
	Cyclohexane carboxylic acid [35]	299.4	265.0	−34.4
	Capric acid [35]	303.9	279.0	−24.9
	Neopentyl alcohol ^{a,b}	328.9	259.2 ^c	−69.7
	Thymol [53]	322.7	271.7	−51.0
	Phenol [54]	313.9	261.3	−52.6
	Neopentyl glycol ^{a,b}	401.2	291.8	−109.4
	Camphor ^a [32]	450.4	275.7	−174.7
	Borneol ^a [32]	480.6	286.7	−193.9
	Sobrerol [32]	420.2	− ^d	−
Choline chloride ^a	Neopentyl glycol ^{a,b}	401.2	305.1	−96.1
	Urea [55]	405.2	297.7	−107.5
Betaine	Urea [56]	405.2	359.3	−45.9
Sulfamic acid	Urea [57]	405.2	351.1	−54.1

Note: ^a plastic crystalline material; ^b measured in this work; ^c ideal eutectic temperature; and ^d the eutectic composition is near pure L-menthol.

Second, three L-menthol-based eutectic systems containing alcohols, i.e., L-menthol/neopentyl alcohol, L-menthol/thymol, and L-menthol/phenol, are compared. L-menthol/thymol and L-menthol/phenol show strong negative deviations from the ideal behavior [53,54]. In contrast, L-menthol/neopentyl alcohol is an ideal eutectic system. As seen in Table 1, the values of ($T_e^{exp} - T_{m,2}$) are considerably small for L-menthol/thymol and L-menthol/phenol. At the same time, L-menthol/neopentyl alcohol shows a significantly low eutectic temperature. Thus, ideal eutectic systems containing PCs can possess lower eutectic temperatures than strongly nonideal eutectic systems.

Third, four eutectic systems containing L-menthol with constituents having high melting temperatures, namely, neopentyl glycol, camphor, borneol, and sobrerol, are compared. As seen in Table 1, the L-menthol/neopentyl glycol, L-menthol/camphor, and L-menthol/borneol eutectic systems show significantly low eutectic temperatures, with ($T_e^{exp} - T_{m,2}$) values of larger than 100 K. In contrast, the eutectic temperature of the L-menthol/sobrerol eutectic system is almost equal to the melting temperature of L-menthol, and its eutectic composition is very close to that of pure L-menthol. This can be attributed to the large difference between the melting temperature of L-menthol and sobrerol [36]. Thus, deep eutectic systems containing constituents that have large differences between their melting temperatures can be formed when the constituent with the high melting temperature is a PC.

ChCl is a PC with a significantly large difference between its solid–plastic transition temperature (351.2 K [13]) and its melting temperature, which should be at least its decomposition temperature (~575 K). This property renders ChCl suitable for forming DESs. The ChCl/urea eutectic system was the first DES that was found to be liquid at room temperature [55]. Urea and neopentyl glycol possess similar melting temperatures; however, urea is not a PC. As seen in Table 1, ChCl/neopentyl glycol shows a similar eutectic temperature and ($T_e^{exp} - T_{m,2}$) value to those of ChCl/urea, forming a liquid solution near room temperature. A comparison of a DES containing betaine or sulfamic acid as an HBA instead of ChCl and urea as an HBD with the ChCl/urea eutectic system revealed that the eutectic temperature of the latter is significantly lower than that of the betaine/urea and sulfamic acid/urea eutectic systems. This clearly emphasizes the unique character of ChCl—and PCs in general—for forming DESs. In conclusion, eutectic systems

showing significant depressions at the eutectic points were obtained using PCs as one or both constituents. The very low melting entropies and enthalpies of the PCs contributed to the significant depressions in the melting temperatures of the mixtures.

3. Materials and Methods

3.1. Eutectic Systems

ChCl ($\geq 98\%$), L-menthol ($\geq 99\%$), neopentyl alcohol ($\geq 99\%$), pivalic acid ($\geq 99\%$), and neopentyl glycol ($\geq 99\%$) were purchased from Merck (Germany). The ChCl and neopentyl glycol were dried under vacuum (~ 1 mbar) at 358 and 313 K, respectively, for at least 24 h. The water content of the pure constituents was checked using a Karl Fischer coulometer (Hanna Instrument, Woonsocket, RI, USA) to ensure that it was below 0.1 wt%. The four eutectic systems, namely, L-menthol/neopentyl alcohol, L-menthol/pivalic acid, L-menthol/neopentyl glycol, and ChCl/neopentyl glycol, were prepared by weighing the pure constituents using a balance (precision 0.1 mg, Sartorius, Germany) and mixing them in sealed vials under heat until clear liquids were formed.

3.2. DSC

The solid–plastic transition and melting properties of the pure PCs and the SLE data were measured using a DSC instrument (NETZSCH DSC 200 F3, Germany), which was calibrated using adamantane, bismuth, cesium chloride, indium, tin, and zinc as the calibration standards. The standard uncertainties of the sensitivity and temperature measurements were determined to be 0.3% and 0.1 K, respectively.

The DSC crucibles were filled in triplicate with the pure PCs. The samples were melted at a heating rate of 5 K min^{-1} , followed by a 5 min isothermal run, and then they were crystallized at a cooling rate of 5 K min^{-1} to a final temperature of 193 K. A second heating run was performed at a rate of 5 K min^{-1} . The transition temperature and the transition enthalpy were determined using the second heating run as the onset temperature and the peak area, respectively. The solid–plastic transition and melting temperatures and enthalpies of neopentyl alcohol, pivalic acid, and neopentyl glycol are shown in Table 2.

Table 2. Transition temperatures (T_{tr}) and enthalpies (Δh_{tr}) and melting temperatures (T_m) and enthalpies (Δh_m) of the studied plastic crystalline materials.

Compound	T_{tr}/K		$\Delta h_{tr}/\text{kJ mol}^{-1}$		T_m/K		$\Delta h_m/\text{kJ mol}^{-1}$	
	This work	Literature	This work	Literature	This work	Literature	This work	Literature
Neopentyl alcohol	235.9 ± 0.1	242.1 ^a	4.46 ± 0.06	4.6 ^a	328.9 ± 1.2	328.1 ^a	4.01 ± 0.03	3.5 ^a
Pivalic acid	279.7 ± 0.1	278.3 ^b	7.99 ± 0.32	8.18 ^b	308.7 ± 0.2	309.1 ^b	2.15 ± 0.13	2.27 ^b
Neopentyl glycol	314.7 ± 0.1	315.2 ^a	12.86 ± 0.20	12.8 ^a	401.2 ± 0.1	402.5 ^a	4.16 ± 0.06	4.3 ^a

Note: ^a data were taken from Granzow [58], and ^b data were taken from Singh and Glicksman [59].

The eutectic system samples were quenched at 198 K for one hour and annealed at 253 K for one day to facilitate the crystallization. The crystallized samples were ground to a fine powder using a mortar and pestle in a cold room at 253 K. The DSC crucibles were filled with the ground solid in triplicates. The solidus and liquidus temperatures of the samples were measured using DSC at a rate of 5 K min^{-1} . The solidus and liquidus temperatures were determined as the onset and peak maximum temperatures of the corresponding peaks, respectively. The experimental SLE data can be found in Tables S1–S4 in the Supplementary Materials.

3.3. SLE Modeling

The experimental SLE data confirmed that the system is of the simple eutectic type. The liquidus line of the components showing no solid–plastic transition was calculated as follows:

$$\ln x_i^L \gamma_i^L = -\frac{\Delta h_{m,i}}{RT} \left(1 - \frac{T}{T_{m,i}}\right) \quad (1)$$

where x_i^L and γ_i^L are the mole fraction and activity coefficients of component i in the liquid phase, respectively; T is the liquidus temperature; $\Delta h_{m,i}$ and $T_{m,i}$ are the melting enthalpy and temperature of component i , respectively; and R is the universal gas constant.

For the PCs, the liquidus line was calculated as follows [60]:

$$\ln x_i^L \gamma_i^L = -\frac{\Delta h_{m,i}}{RT} \left(1 - \frac{T}{T_{m,i}}\right) - \frac{\Delta h_{tr,i}}{RT} \left(1 - \frac{T}{T_{tr,i}}\right) \quad (2)$$

where $\Delta h_{tr,i}$ and $T_{tr,i}$ are the solid–plastic transition enthalpy and temperature of component i , respectively.

The SLE phase diagram of the L-menthol-based eutectic systems was calculated assuming the ideal solution model, i.e., $\gamma_i^L = 1$, using Equations (1) and (2) for the L-menthol and the PCs, respectively. The solid–plastic transition and melting properties of the PCs measured in this work (Table 2) were used, and those of L-menthol were taken from the literature ($T_{m,i} = 314.6$ K and $\Delta h_{m,i} = 13.74$ kJ mol^{−1} [35]).

The ChCl/neopentyl glycol eutectic system showed a negative deviation from the ideal behavior. The activity coefficients of neopentyl glycol in the ChCl/neopentyl glycol eutectic system were calculated using the following Redlich–Kister polynomial equation, with one parameter [61]:

$$\ln \gamma_i^L = \frac{A}{RT} (1 - x_i) \quad (3)$$

The binary interaction parameter A was fitted to the neopentyl glycol experimental liquidus data (T_i^{exp}), minimizing the following objective function:

$$F(T) = \sum_{i=1}^n \left(\frac{(T_i^{exp} - T_i^{cal})^2}{n} \right)^{\frac{1}{2}} \quad (4)$$

where n is the number of data points. The calculated binary interaction parameter A was -2.9192 kJ mol^{−1}.

4. Conclusions

This work demonstrates the formation of eutectic systems with low eutectic temperatures using PCs as constituents. Three PCs having chemical natures resembling common HBDs used in the DES literature, namely, monocarboxylic acids, alcohols, and diols, were selected in this work. The solid–plastic transition and melting properties of the three PCs were measured using DSC. The SLE phase diagrams of four eutectic systems containing the three PCs and L-menthol or ChCl were determined via DSC and modeled using the ideal solution model and Redlich–Kister polynomial equation (with one parameter).

The SLE phase diagrams reported in this work showed that PCs can form eutectic systems with large depressions at the eutectic points relative to the melting temperatures of the pure constituents. Despite having melting temperatures significantly higher than those of their structural isomers, the PCs possess very low melting enthalpies and entropies, increasing the slopes of the liquidus lines of the pure constituents above the solid–plastic transition temperatures and resulting in low eutectic temperatures. However, because the solid–plastic transition enthalpies are larger than the melting enthalpies of the PCs, the slopes of the liquidus lines below the solid–plastic transition temperatures become less

steep. Hence, PCs with large differences between the solid–plastic transition temperatures and the melting temperatures were found to form deeper eutectics.

Despite the nearly ideal behavior observed in the studied systems, the eutectic temperature depressions were comparable or even larger than those observed in strongly nonideal eutectic systems containing common crystalline solids. For practical applications, it is more important to have a DES that is liquid and lowly viscous at the operating conditions independent of the nonideality of the system. Thus, ideal eutectic systems containing PCs could be promising green solvents for various applications.

Supplementary Materials: The following supporting information can be downloaded at: <https://www.mdpi.com/article/10.3390/molecules27196210/s1>, Table S1. Solid–liquid equilibria data of the L-menthol/neopentyl alcohol eutectic system. Table S2. Solid–liquid equilibria data of the L-menthol/pivalic acid eutectic system. Table S3. Solid–liquid equilibria data of the L-menthol/neopentyl glycol eutectic system. Table S4. Solid–liquid equilibria data of the ChCl/neopentyl alcohol eutectic system.

Author Contributions: Conceptualization, A.A.; methodology, A.A.; formal analysis, A.A. and S.N.; investigation, A.A. and S.N.; writing—original draft preparation, A.A.; writing—review and editing, L.M. and M.M.; supervision, M.M. All authors have read and agreed to the published version of the manuscript.

Funding: This work was supported by the German Research Foundation (DFG) and the Technical University of Munich (TUM) in the framework of the Open Access Publishing Program.

Institutional Review Board Statement: Not applicable.

Informed Consent Statement: Not applicable.

Data Availability Statement: All data supporting the reported results can be found within the manuscript and the Supplementary Materials.

Acknowledgments: S.N. would like to thank the German Academic Exchange Service (DAAD) for financial support.

Conflicts of Interest: The authors declare no conflict of interest.

Sample Availability: Samples of the studied compounds and mixtures are unavailable.

References

1. Smith, E.L.; Abbott, A.P.; Ryder, K.S. Deep Eutectic Solvents (DESs) and Their Applications. *Chem. Rev.* **2014**, *114*, 11060–11082. [[CrossRef](#)] [[PubMed](#)]
2. Zhang, Q.; De Oliveira Vigier, K.; Royer, S.; Jerome, F. Deep eutectic solvents: Syntheses, properties and applications. *Chem. Soc. Rev.* **2012**, *41*, 7108–7146. [[CrossRef](#)] [[PubMed](#)]
3. Wazeer, I.; Hadj-Kali, M.K.; Al-Nashef, I.M. Utilization of Deep Eutectic Solvents to Reduce the Release of Hazardous Gases to the Atmosphere: A Critical Review. *Molecules* **2021**, *26*, 75. [[CrossRef](#)] [[PubMed](#)]
4. Winterton, N. The green solvent: A critical perspective. *Clean Technol. Environ. Policy* **2021**, *23*, 2499–2522. [[CrossRef](#)]
5. Florindo, C.; Branco, L.C.; Marrucho, I.M. Quest for Green-Solvent Design: From Hydrophilic to Hydrophobic (Deep) Eutectic Solvents. *ChemSusChem* **2019**, *12*, 1549–1559. [[CrossRef](#)]
6. Abranches, D.O.; Coutinho, J.A.P. Type V deep eutectic solvents: Design and applications. *Curr. Opin. Green Sustain. Chem.* **2022**, *35*, 100612. [[CrossRef](#)]
7. Perna, F.M.; Vitale, P.; Capriati, V. Deep eutectic solvents and their applications as green solvents. *Curr. Opin. Green Sustain. Chem.* **2020**, *21*, 27–33. [[CrossRef](#)]
8. Dheyab, A.S.; Bakar, M.F.A.; Alomar, M.; Sabran, S.F.; Hanafi, A.F.M.; Mohamad, A. Deep eutectic solvents (DESs) as green extraction media of beneficial bioactive phytochemicals. *Separations* **2021**, *8*, 176. [[CrossRef](#)]
9. Huang, J.; Guo, X.; Xu, T.; Fan, L.; Zhou, X.; Wu, S. Ionic deep eutectic solvents for the extraction and separation of natural products. *J. Chromatogr. A* **2019**, *1598*, 1–19. [[CrossRef](#)]
10. Álvarez, M.S.; Zhang, Y. Sketching neoteric solvents for boosting drugs bioavailability. *J. Control Release* **2019**, *311–312*, 225–232. [[CrossRef](#)]
11. Hou, Y.; Congfei, Y.; Weize, W. Deep Eutectic Solvents: Green Solvents for Separation Applications. *Acta Phys.-Chim. Sin.* **2018**, *34*, 873–885. [[CrossRef](#)]

12. Florindo, C.; Romero, L.; Rintoul, I.; Branco, L.C.; Marrucho, I.M. From Phase Change Materials to Green Solvents: Hydrophobic Low Viscous Fatty Acid-Based Deep Eutectic Solvents. *ACS Sustain. Chem. Eng.* **2018**, *6*, 3888–3895. [[CrossRef](#)]
13. Alhadid, A.; Jandl, C.; Mokrushina, L.; Minceva, M. Cocrystal Formation in Choline Chloride Deep Eutectic Solvents. *Cryst. Growth Des.* **2022**, *22*, 1933–1942. [[CrossRef](#)]
14. Andruch, V.; Makoš-Chelstowska, P.; Plotka-Wasyłka, J. Remarks on use of the term “deep eutectic solvent” in analytical chemistry. *Microchem. J.* **2022**, *179*, 107498. [[CrossRef](#)]
15. Crespo, E.A.; Silva, L.P.; Martins, M.A.R.; Bülow, M.; Ferreira, O.; Sadowski, G.; Held, C.; Pinho, S.P.; Coutinho, J.A.P. The Role of Polyfunctionality in the Formation of [Ch]Cl-Carboxylic Acid-Based Deep Eutectic Solvents. *Ind. Eng. Chem. Res.* **2018**, *57*, 11195–11209. [[CrossRef](#)]
16. van den Bruinhorst, A.; Kollau, L.J.B.M.; Vis, M.; Hendrix, M.M.R.M.; Meuldijk, J.; Tuinier, R.; Esteves, A.C.C. From a eutectic mixture to a deep eutectic system via anion selection: Glutaric acid + tetraethylammonium halides. *J. Chem. Phys.* **2021**, *155*, 014502. [[CrossRef](#)] [[PubMed](#)]
17. Kollau, L.J.B.M.; Tuinier, R.; Verhaak, J.; den Doelder, J.; Filot, I.A.W.; Vis, M. Design of Nonideal Eutectic Mixtures Based on Correlations with Molecular Properties. *J. Phys. Chem. B* **2020**, *124*, 5209–5219. [[CrossRef](#)]
18. Silva, L.P.; Martins, M.A.R.; Conceição, J.H.F.; Pinho, S.P.; Coutinho, J.A.P. Eutectic Mixtures Based on Polyalcohols as Sustainable Solvents: Screening and Characterization. *ACS Sustain. Chem. Eng.* **2020**, *8*, 15317–15326. [[CrossRef](#)]
19. Silva, L.P.; Fernandez, L.; Conceição, J.H.F.; Martins, M.A.R.; Sosa, A.; Ortega, J.; Pinho, S.P.; Coutinho, J.A.P. Design and Characterization of Sugar-Based Deep Eutectic Solvents Using Conductor-like Screening Model for Real Solvents. *ACS Sustain. Chem. Eng.* **2018**, *6*, 10724–10734. [[CrossRef](#)]
20. Silva, L.P.; Martins, M.A.R.; Abranches, D.O.; Pinho, S.P.; Coutinho, J.A.P. Solid-liquid phase behavior of eutectic solvents containing sugar alcohols. *J. Mol. Liq.* **2021**, *337*, 116392. [[CrossRef](#)]
21. Silva, L.P.; Araújo, C.F.; Abranches, D.O.; Melle-Franco, M.; Martins, M.A.R.; Nolasco, M.M.; Ribeiro-Claro, P.J.A.; Pinho, S.P.; Coutinho, J.A.P. What a difference a methyl group makes—probing choline–urea molecular interactions through urea structure modification. *PCCP* **2019**, *21*, 18278–18289. [[CrossRef](#)] [[PubMed](#)]
22. van den Bruinhorst, A.; Kollau, L.J.B.M.; Kroon, M.C.; Meuldijk, J.; Tuinier, R.; Esteves, A.C.C. A centrifuge method to determine the solid–liquid phase behavior of eutectic mixtures. *J. Chem. Phys.* **2018**, *149*, 224505. [[CrossRef](#)] [[PubMed](#)]
23. Hayyan, M.; Looi, C.Y.; Hayyan, A.; Wong, W.F.; Hashim, M.A. In Vitro and In Vivo Toxicity Profiling of Ammonium-Based Deep Eutectic Solvents. *PLoS ONE* **2015**, *10*, e0117934. [[CrossRef](#)]
24. Wazeer, I.; AlNashef, I.M.; Al-Zahrani, A.A.; Hadj-Kali, M.K. The subtle but substantial distinction between ammonium- and phosphonium-based deep eutectic solvents. *J. Mol. Liq.* **2021**, *332*, 115838. [[CrossRef](#)]
25. Gajardo-Parra, N.F.; Cotroneo-Figueroa, V.P.; Aravena, P.; Vesovic, V.; Canales, R.I. Viscosity of Choline Chloride-Based Deep Eutectic Solvents: Experiments and Modeling. *J. Chem. Eng. Data* **2020**, *65*, 5581–5592. [[CrossRef](#)]
26. Lemaoui, T.; Darwish, A.S.; Attoui, A.; Abu Hatab, F.; Hammoudi, N.E.H.; Benguerba, Y.; Vega, L.F.; Alnashef, I.M. Predicting the density and viscosity of hydrophobic eutectic solvents: Towards the development of sustainable solvents. *Green Chem.* **2020**, *22*, 8511–8530. [[CrossRef](#)]
27. Al-Dawsari, J.N.; Bessadok-Jemai, A.; Wazeer, I.; Mokraoui, S.; AlMansour, M.A.; Hadj-Kali, M.K. Fitting of experimental viscosity to temperature data for deep eutectic solvents. *J. Mol. Liq.* **2020**, *310*, 113127. [[CrossRef](#)]
28. Mjalli, F.S.; Naser, J. Viscosity model for choline chloride-based deep eutectic solvents. *Asia-Pac. J. Chem. Eng.* **2015**, *10*, 273–281. [[CrossRef](#)]
29. van Osch, D.J.G.P.; Dietz, C.H.J.T.; van Spronsen, J.; Kroon, M.C.; Gallucci, F.; van Sint Annaland, M.; Tuinier, R. A Search for Natural Hydrophobic Deep Eutectic Solvents Based on Natural Components. *ACS Sustain. Chem. Eng.* **2019**, *7*, 2933–2942. [[CrossRef](#)]
30. Aşçı, Y.S.; Lalikoglu, M. Development of New Hydrophobic Deep Eutectic Solvents Based on Trioctylphosphine Oxide for Reactive Extraction of Carboxylic Acids. *Ind. Eng. Chem. Res.* **2021**, *60*, 1356–1365. [[CrossRef](#)]
31. Abdallah, M.M.; Müller, S.; González de Castilla, A.; Gurikov, P.; Matias, A.A.; Bronze, M.D.; Fernández, N. Physicochemical Characterization and Simulation of the Solid–Liquid Equilibrium Phase Diagram of Terpene-Based Eutectic Solvent Systems. *Molecules* **2021**, *26*, 1801. [[CrossRef](#)] [[PubMed](#)]
32. Martins, M.A.R.; Silva, L.P.; Schaeffer, N.; Abranches, D.O.; Maximo, G.J.; Pinho, S.P.; Coutinho, J.A.P. Greener Terpene–Terpene Eutectic Mixtures as Hydrophobic Solvents. *ACS Sustain. Chem. Eng.* **2019**, *7*, 17414–17423. [[CrossRef](#)]
33. Alhadid, A.; Safarov, J.; Mokrushina, L.; Müller, K.; Minceva, M. Carbon Dioxide Solubility in Nonionic Deep Eutectic Solvents Containing Phenolic Alcohols. *Front. Chem.* **2022**, *10*, 300. [[CrossRef](#)] [[PubMed](#)]
34. Alhadid, A.; Mokrushina, L.; Minceva, M. Influence of the Molecular Structure of Constituents and Liquid Phase Non-Ideality on the Viscosity of Deep Eutectic Solvents. *Molecules* **2021**, *26*, 4208. [[CrossRef](#)]
35. Alhadid, A.; Mokrushina, L.; Minceva, M. Design of Deep Eutectic Systems: A Simple Approach for Preselecting Eutectic Mixture Constituents. *Molecules* **2020**, *25*, 1077. [[CrossRef](#)]
36. Alhadid, A.; Mokrushina, L.; Minceva, M. Modeling of Solid–Liquid Equilibria in Deep Eutectic Solvents: A Parameter Study. *Molecules* **2019**, *24*, 2334. [[CrossRef](#)]
37. Das, S.; Mondal, A.; Reddy, C.M. Harnessing molecular rotations in plastic crystals: A holistic view for crystal engineering of adaptive soft materials. *Chem. Soc. Rev.* **2020**, *49*, 8878–8896. [[CrossRef](#)]

38. Alarco, P.-J.; Abu-Lebdeh, Y.; Abouimrane, A.; Armand, M. The plastic-crystalline phase of succinonitrile as a universal matrix for solid-state ionic conductors. *Nat. Mater.* **2004**, *3*, 476–481. [[CrossRef](#)]
39. Timmermans, J. Plastic crystals: A historical review. *J. Phys. Chem. Solids* **1961**, *18*, 1–8. [[CrossRef](#)]
40. Lohmann, J.; Joh, R.; Gmehling, J. Solid–Liquid Equilibria of Viscous Binary Mixtures with Alcohols. *J. Chem. Eng. Data* **1997**, *42*, 1170–1175. [[CrossRef](#)]
41. Parks, G.S.; Huffman, H.M.; Barmore, M. Thermal data on organic compounds. XI. The heat capacities, entropies and free energies of ten compounds containing oxygen or nitrogen. *J. Am. Chem. Soc.* **1933**, *55*, 2733–2740. [[CrossRef](#)]
42. Timmermans, J. Freezing points of organic compounds. VVI New determinations. *Bull. Soc. Chim. Belg.* **1952**, *61*, 393–402. [[CrossRef](#)]
43. Miller, P. *The Free Energy of Furfural and Some of Its Derivatives*; Iowa State University: Ames, IA, USA, 1934.
44. Mellan, I. *Polyhydric Alcohols*; Spartan Books: Washington, DC, USA, 1962.
45. Jain, A.; Yang, G.; Yalkowsky, S.H. Estimation of Total Entropy of Melting of Organic Compounds. *Ind. Eng. Chem. Res.* **2004**, *43*, 4376–4379. [[CrossRef](#)]
46. Sherwood, J.N. *The Plastically Crystalline State: Orientationally Disordered Crystals*; John Wiley & Sons: Hoboken, NJ, USA, 1979.
47. Alizadeh, V.; Malberg, F.; Pádua, A.A.H.; Kirchner, B. Are There Magic Compositions in Deep Eutectic Solvents? Effects of Composition and Water Content in Choline Chloride/Ethylene Glycol from Ab Initio Molecular Dynamics. *J. Phys. Chem. B* **2020**, *124*, 7433–7443. [[CrossRef](#)] [[PubMed](#)]
48. Li, G.; Deng, D.; Chen, Y.; Shan, H.; Ai, N. Solubilities and thermodynamic properties of CO₂ in choline-chloride based deep eutectic solvents. *J. Chem. Thermodyn.* **2014**, *75*, 58–62. [[CrossRef](#)]
49. Spittle, S.; Poe, D.; Doherty, B.; Kolodziej, C.; Heroux, L.; Haque, M.A.; Squire, H.; Cosby, T.; Zhang, Y.; Fraenza, C.; et al. Evolution of microscopic heterogeneity and dynamics in choline chloride-based deep eutectic solvents. *Nat. Commun.* **2022**, *13*, 219. [[CrossRef](#)]
50. Agieienko, V.; Buchner, R. Correction: Is ethaline a deep eutectic solvent? *PCCP* **2022**, *24*, 10628. [[CrossRef](#)]
51. Crespo, E.A.; Silva, L.P.; Lloret, J.O.; Carvalho, P.J.; Vega, L.F.; Llovel, F.; Coutinho, J.A.P. A methodology to parameterize SAFT-type equations of state for solid precursors of deep eutectic solvents: The example of cholinium chloride. *PCCP* **2019**, *21*, 15046–15061. [[CrossRef](#)]
52. Agieienko, V.; Buchner, R. Is ethaline a deep eutectic solvent? *PCCP* **2022**, *24*, 5265–5268. [[CrossRef](#)]
53. Alhadid, A.; Jandl, C.; Mokrushina, L.; Minceva, M. Experimental Investigation and Modeling of Cocrystal Formation in L-Menthol/Thymol Eutectic System. *Cryst. Growth Des.* **2021**, *21*, 6083–6091. [[CrossRef](#)]
54. Alhadid, A.; Jandl, C.; Mokrushina, L.; Minceva, M. Cocrystal Formation in l-Menthol/Phenol Eutectic System: Experimental Study and Thermodynamic Modeling. *Cryst. Growth Des.* **2022**, *22*, 3973–3980. [[CrossRef](#)]
55. Meng, X.; Ballerat-Busserolles, K.; Husson, P.; Andanson, J.-M. Impact of water on the melting temperature of urea + choline chloride deep eutectic solvent. *New J. Chem.* **2016**, *40*, 4492–4499. [[CrossRef](#)]
56. Abranches, D.O.; Silva, L.P.; Martins, M.A.R.; Pinho, S.P.; Coutinho, J.A.P. Understanding the Formation of Deep Eutectic Solvents: Betaine as a Universal Hydrogen Bond Acceptor. *ChemSusChem* **2020**, *13*, 4916–4921. [[CrossRef](#)]
57. Kazachenko, A.S.; Issaoui, N.; Medimagh, M.; Fetisova, O.Y.; Berezhnaya, Y.D.; Elsufev, E.V.; Al-Dossary, O.M.; Wojcik, M.J.; Xiang, Z.; Bousiakou, L.G. Experimental and theoretical study of the sulfamic acid-urea deep eutectic solvent. *J. Mol. Liq.* **2022**, *363*, 119859. [[CrossRef](#)]
58. Granzow, B. Hydrogen bonding and phase transitions of a group of alcohols derived from 2,2-dimethylpropane. *J. Mol. Struct.* **1996**, *381*, 127–131. [[CrossRef](#)]
59. Singh, N.B.; Glicksman, M.E. Physical properties of ultra-pure pivalic acid. *Thermochim. Acta* **1990**, *159*, 93–99. [[CrossRef](#)]
60. Lohmann, J.; Joh, R.; Gmehling, J. Estimation of Enthalpies of Fusion, Melting Temperatures, Enthalpies of Transition, and Transition Temperatures of Pure Compounds from Experimental Binary Solid–Liquid Equilibrium Data of Eutectic Systems. *J. Chem. Eng. Data* **1997**, *42*, 1176–1180. [[CrossRef](#)]
61. Prausnitz, J.M.; Lichtenthaler, R.N.; de Azevedo, E.G. *Molecular Thermodynamics of Fluid-Phase Equilibria*; Prentice Hall PTR: Upper Saddle River, NJ, USA, 1999.